Green Synthesis of Iron Oxide, and Iron Oxide/ Cerium Oxide Nanoparticles Using *Ficus nitida* Extract: Antimicrobial and Antioxidant Activities

Mostafa I. Abdelglil,[a] Naifa Alenazi,[b] Abdullah A. Saber,[c] Amani Alhejely,[d] Mohamed H. El-Sayed,[e] Salama A. Salama,[f] Mohamed A. Amin,[g,*] and Mohamed H. Sharaf [g]

To minimize environmental impact, the green synthesis strategy prioritized using non-toxic substances, energy-efficient processes, and renewable resources. *Ficus nitida* fruit extract was used to produce Iron oxide nanoparticles (Fe_2O_3 and Fe_3O_4 NPs) and Iron oxide/cerium oxide nanoparticles (Fe_2O_3 and Fe_3O_4/CeO_2 NPs) for antimicrobial, and antioxidant applications. The effective synthesis of these NPs was confirmed by X-ray diffraction (XRD), FTIR, UV-visible, and transmission electron microscopic (TEM) analyses. The typical crystal diameters, as estimated by the Debye–Scherrer equation, were 3.65 nm (Fe_2O_3 and Fe_3O_4 NPs) and 10.14 nm (Fe_2O_3 and Fe_3O_4/CeO_2 NPs). TEM images verified that the prepared NPs were spherical, semispherical, and irregular in shape. The FTIR spectrum's prominent peaks revealed the elements of Fe–Ce nanoparticles. Of all the materials examined, Fe_2O_3 and Fe_3O_4 /CeO_2 NPs synthesized using *Ficus nitida* fruit extract demonstrated promising in vitro antibacterial activity against MRSA (21.0 ± 0.58 mm inhibition zone) and *E. coli* (22.2 ± 0.15 mm), alongside antioxidant potential (81.76% free radical scavenging at 1000 µg/mL). These preliminary findings merit further investigation to assess toxicity, biocompatibility, and *in vivo* efficacy as potential antibacterial and antioxidant agents in advanced applications.

DOI: 10.15376/biores.21.2.3673-3687

Keywords: Iron oxide; Cerium oxide nanoparticles; Ficus nitida fruits; Antimicrobial and antioxidant activities

Contact information a: College of Pharmacy, Al-Farahidi University-Baghdad-Iraq; b: Department of Pharmaceutical Sciences, College of Pharmacy, Princess Nourah bint Abdulrahman University, P.O. Box 84428, Riyadh 11671, Saudi Arabia; c: Biology Department, College of Science, Imam Mohammad Ibn Saud Islamic University (IMSIU), Riyadh 11623,Saudi Arabia; d: Biology Department, Darb University College, Jazan University, Saudi Arabia; e: Department of Biological Sciences, College of Science, Northern Border University, Arar, Saudi Arabia; f: Biology Department, Faculty of Science, Jazan University, P.O. Box 114, Jazan 45142, Saudi Arabia; g: Botany and Microbiology Department, Faculty of Science, Al-Azhar University Cairo 11884, Egypt;

** Corresponding author: mamin7780@azhar.edu.eg*

INTRODUCTION

Nanoparticles can alter the physicochemical reactions of many chemicals, which can significantly affect the biology of existing cells. Given the wide range of sizes and shapes of these entities, it is difficult to forecast the positive or negative effects and their mechanisms of action in biological systems and the environment (Chen *et al*. 2020). The creation and use of nanotechnology have affected several industries, including the

manufacturing of medications and food. To ensure the sustainable and optimal use of these items, it is crucial to comprehend their benefits and drawbacks (Abdelghany *et al*. 2023; El-Batal *et al*. 2023; Amin *et al*. 2024, 2025; Abd-ElGawad *et al*. 2025).

Because of their unique electrical, optical, and magnetic characteristics, nanoparticles (NPs) have garnered a lot of interest (Selim *et al*. 2025). Certain physicochemical properties, such as a high surface-to-volume ratio, are produced using nanotechnology. Discovering, characterizing, and modifying the special qualities of matter at the nanoscale is another goal of nanotechnology, which aims to create new capabilities with possible uses in all branches of science, engineering, technology, and medicine. Because of their numerous uses in fields including coatings, packaging, electronics, cosmetics, and biotechnology, metallic NPs are being researched extensively (Dikshit *et al*. 2021).

The increasing prevalence of antibiotic-resistant bacteria has become one of the most serious challenges in modern medicine. Traditional antibiotics are losing effectiveness, which motivates the search for novel antimicrobial agents that are safer, more sustainable, and less prone to resistance development. In recent years, combining natural products-especially plant extracts-with nanotechnology has emerged as a promising strategy, because plant-derived metabolites can act as reducing and capping agents for nanoparticle synthesis, while metallic NPs themselves can exert antibacterial effects through physical and chemical mechanisms (Radulescu *et al*. 2023).

Species in the genus *Ficus* are known to produce a variety of secondary metabolites-flavonoids, phenolic acids, tannins, alkaloids, and terpenoids—that have antioxidant, anti-inflammatory, and antimicrobial properties. Although *Ficus nitida* is less frequently studied than other *Ficus* species, the general bioactivity reported for *Ficus* plant extracts suggests that *Ficus nitida* may also harbor bioactive compounds capable of inhibiting bacterial growth. In green synthesis protocols, extracts from *Ficus* species have potential to reduce and stabilize metal ions into NPs through the functional groups such as hydroxyl and carbonyl groups that donate electrons and coordinate metal ions (Shreyash *et al*. 2021; Singh *et al*. 2023).

Iron-based nanoparticles, especially iron oxides NPs, are among the promising nanomaterials in antibacterial research because of their catalytic and redox properties. They can generate reactive oxygen species (ROS), liberate iron ions (Fe^{2+}/Fe^{3+}), and physically interact with bacterial cell surfaces, all contributing to bacterial cell damage or death. The antibacterial effectiveness of these NPs typically depends on parameters such as particle size, surface charge, morphology, and degree of aggregation. Smaller, well-dispersed particles with higher surface area usually present stronger antibacterial action (Nadeem *et al*. 2021; Radulescu *et al*. 2023).

Cerium, especially in its oxide form (CeO_2 or mixed metal forms with Fe), exhibits unique redox cycling between Ce^{3+} and Ce^{4+}. This redox flexibility can confer antimicrobial behavior: the reversible conversion can mediate oxidative stress, scavenge radicals, and disrupt microbial homeostasis. Pure cerium oxide nanoparticles (CeO_2 NPs) have been explicitly studied for antimicrobial effects, with observed activity against bacteria such as *Pseudomonas aeruginosa* (Qi *et al*. 2020; Zamani *et al*. 2021).

Using *Ficus nitida* fruits extract as a bioreducing and capping agent for synthesizing Fe and Fe–Ce NPs is expected to yield "green" nanocomposites that combine phytochemical-driven bioactivity with nanoparticle-mediated antimicrobial mechanisms. The plant extract may support nanoparticle stability, prevent aggregation, and contribute additional antimicrobial effects (Vijayaram *et al*. 2024).

In previous reports, iron oxide nanoparticles have been synthesized using extracts from other plants, including *Ficus carica* fruits (Demirezen *et al*. 2019). In contrast, the present study is, to the authors' knowledge, the first to employ *Ficus nitida* fruit extract to simultaneously synthesize FeO, and FeO/CeO_2 nanocomposites and to systematically evaluate their in vitro antibacterial and antioxidant activities, linking the specific phytochemical profile of *F. nitida* fruits to the observed bioactivity. This study advances previous work by (i) introducing a new *Ficus* species (*F. nitida*) and plant part (fruit) as a green reducing and capping agent, (ii) generating a Fe–Ce bimetallic oxide nanohybrid not previously reported with this extract, and (iii) focusing on dual antibacterial–antioxidant functionality as a basis for future biomedical exploration, rather than single-property evaluation.

EXPERIMENTAL

Ficus nitida Fruits Extract

Ficus nitida fruits were collected from the Botanical Garden in Al-Qanater El-Khyria, El-Qulyubia Governorate, Egypt. After being cleaned with distilled water, the fruits were left to air dry for two weeks before being ground into a powder. About 5 g of air-dried powder and 100 mL of distilled water were combined, and the mixture was sonicated for two hours at 50 °C in a water bath to create the fruit aqueous extract. The extract was then filtered through Whatman No. 1 filter paper and the filtrate obtained was stored in a refrigerator at 4 °C.

Synthesis of FeO and FeO/CeO NPs

First, 3 g of ferrous sulphate ($FeSO_4.7H_2O$) was added to 100 mL of fruits extract, while stirring continuously at 400 rpm. For two hours, a mixture of salt and extract was heated at 70 °C constantly on a hot plate. The pH of the reaction mixture was found to be 9. The synthesis of Fe-NPs was verified by a change in liquid color. To separate the NPs from the solution, centrifugation was carried out at 3000 rpm for 30 minutes. The NPs pellet was cleaned three- or four-times using double-distilled water to remove impurities (Yekeen *et al*. 2025). The same method used to create bimetallic oxides (FeO/CeO NPs) by using 3 g of ferrous sulphate ($FeSO_4.7H_2O$) and $Ce(NO_3)_3 \cdot 6H_2O$.

Characterization of the FeO and FeO/CeO NPs

The X-ray diffraction (XRD) patterns of the FeO and FeO/CeO NPs were examined using Cu Kα radiation (λ=1.5406 Å) with a range of 2θ° from 20° to 80° at a scanning rate of 0.02° in a Bruker D8 Discover X-ray diffractometer. Transmission electron microscopy (TEM) images of these NPs were obtained using a JEM-2100 PLUS electron microscope (JEOL, Japan) running at 200 kV with a LaB6 source. The functional groups that are shared in the production of NPs are identified using FTIR spectra. UV-Vis was used to monitor the synthesized FeO NPs and FeO/CeO NPs in the 100 to 900 nm range. A UV-Visible Jasco V-550 spectrophotometer was used to record the UV-visible spectra **(**Selim *et al.* 2025 a,b**)**

Antimicrobial Activity

The antibacterial potential of the plant extract, Fe-NPs and Consortium (Fe/Ce NPs) were evaluated using the agar well diffusion method. Multidrug resistant Bacterial strains

tested included MRSA, *Bacillus cereus, Staphylococcus aureus*, *Klebsiella pneumoniae*, *Escherichia coli*, and *Acinetobacter baumannii*. Wells were filled with 100 µL of each sample (1 mg/mL concentration). Erythromycin disk 15 µg was used as a standard antibiotic control. Plates were incubated at 37 °C for 24 h, and the zones of inhibition (mm) were measured. Each test was performed in triplicate, and results were expressed as mean ± SE**.** (Sharaf *et al*. 2021).

Determination of Minimum Inhibitory Concentration (MIC)

MIC values of Fe-NPs and Consortium (Fe/Ce NPs) were performed against MRSA, *Bacillus cereus*, *Staphylococcus aureus*, *Klebsiella pneumoniae*, *Escherichia coli*, and *Acinetobacter baumannii*, following the method of El-Didamony *et al*. (2024).

Antioxidant Activity

DPPH assay

Antioxidant activity of Fe-NPs and consortium (Fe/Ce NPs) were carried out using DPPH (2, 2-diphenyl-1-picrylhydrazyl) method according to El-Sayed *et al.* (2023) with minor modifications. DPPH assay was performed following standard protocol (0.1 mM DPPH in methanol, 100 µL NP samples at 31.25-1000 µg/mL). To minimize nanoparticle-specific artifacts including Mie scattering, optical interference at 517 nm, and metal ion interference with DPPH chromophore, samples were centrifuged (10,000 × g, 10 min) prior to reading to remove suspended NPs while retaining soluble antioxidant metabolites in supernatant. Absorbance was measured at 517 nm. Percentage inhibition was calculated relative to methanol-blank. The NPs supernatant blanks were corrected to account for baseline absorbance. Ascorbic acid served as the standard control, although its mechanism differs significantly from that of metal oxide nanoparticles.

Statistical Analysis

Minitab 18 was used for statistical calculations at the 0.05 level of probability. Quantitative data having parametric distribution was examined using one-way ANOVA, post hoc Tukey's test, and analyses of variance.

RESULTS and DISCUSSION

Characterization of FeO and FeO/CeO NPs

TEM and UV spectrum

In this study, the synthesis of biogenic Fe NPs and Fe/Ce NPs using *Ficus nitida* fruits extract was demonstrated by a shift in the color of the solution, which served as both a capping and reducing agent. The plant extract appeared pale in color; it turned dark brown (Fe NPs) and red (Fe/Ce NPs). In accordance with the UV-Vis. Studies have shown that the Fe NPs are tiny and visible at 261 and 284 nm, while the Fe/Ce NPs are visible at 257nm (Fig. 1c and d). The HR-TEM image (Fig. 1a, b) showed the spheroidal and semispherical shapes and had a typical size between 42.52 and 83.10 nm for Fe NPs and between 27.17 and 74.17 nm for Fe/Ce NPs**.**

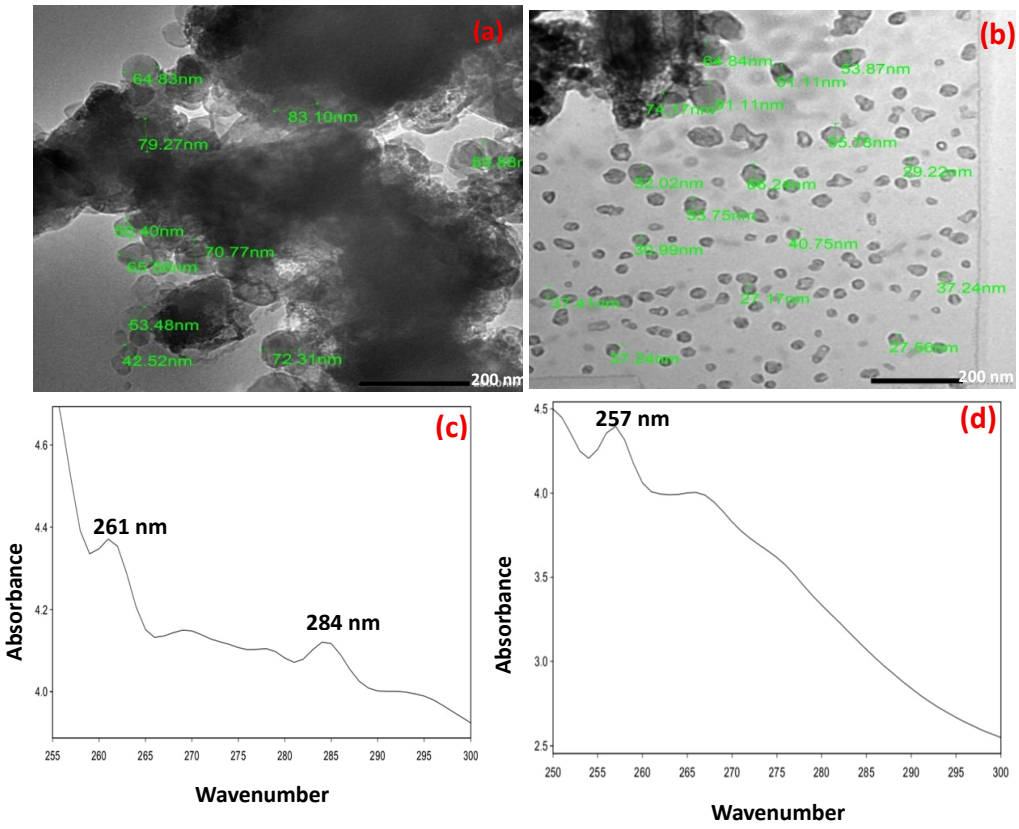

Fig. 1. TEM image (a,b), and UV spectrum (c,d) of Fe-NPs and Fe/Ce NPs respectively

FTIR analysis

Figures 2a and 2b show the different functional groups of fruit extract used in NPs synthesis. The IR chart suggests that the bioactive molecules, including hydroxyl, carbonyl amides, and amines, found in the plant extract remain attached or coated on the surface of NPs, enhancing their stability. FT-IR measurements were conducted to complement the materials characterization (Figs. 2c, 2d).

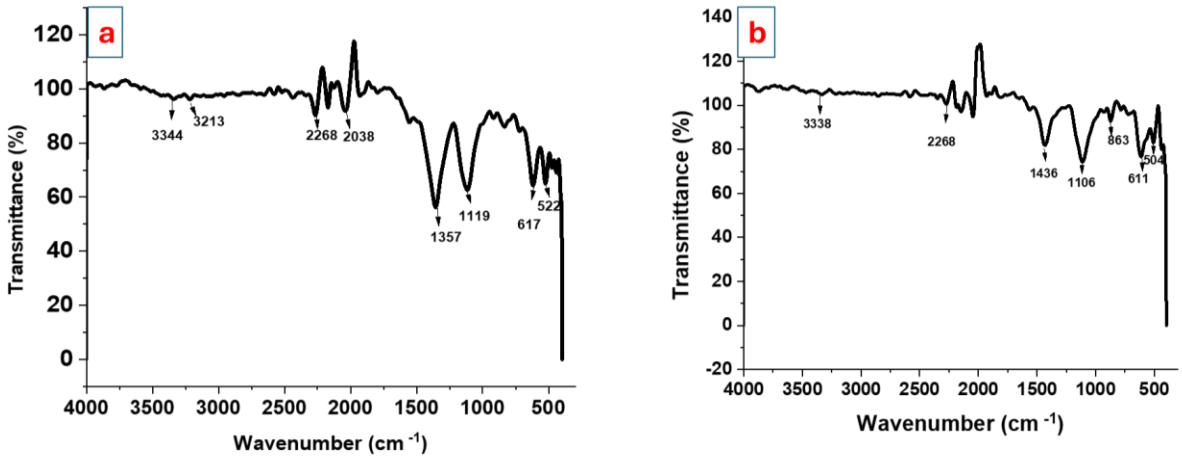

Fig. 2. FTIR analysis of FeO NPs (a); and FeO/CeO NPs (b)

The spectrum of Fe-NPs and Fe/Ce NPs showed bands at 522 and 617 cm^{-1} attributed to vibrations of the symmetric stretching of Fe–O bond (Sriram *et al*. 2022). The Ce-O vibrations were identified by a band at 863 cm^{-1} in the Fe/Ce NPs spectra, while the peaks at 1337 and 1436 cm^{-1} are associated with CeO_2 (Rego *et al*. 2021). According to Basu *et al*. (2013), these groups help produce the bimetallic oxyhydroxides (Ce–O–Fe), which are a feature of the synthetic metal oxides Ce–OH and Fe–OH seen at 1106 cm^{-1}. Aromatic C–H bending, allene C=C=C stretching, or alkyne C–C stretching may be associated with the intensity and appearance or disappearance of peaks between 2268 and 2038 cm^{-1} (Salih *et al*. 2023). The O–H bending carboxylic acid group is shown by a peak at 1357 cm^{-1} (Mohamed *et al*. 2022). Some functional compounds such as amine ($-NH_2$), carboxyl (-COOH), or hydroxyl (-OH) groups operate as capping agents to improve the stability of nanoparticles against aggregation (Pedroso-Santana and Fleitas-Salazar (2023)).

XRD analysis

The crystallography of nano- FeO synthesized from plants was examined *via* X-ray diffraction (XRD). The XRD chart (Fig. 3a) shows that the various Bragg diffraction peaks of (012), (030), (104), (025) (110), (024), and (214) emerged at 2θ° values of 23.3°, 29.57°, 32.05°, 34.04°, 35. 6°, 38.95°, 48.23°, and 62. 8°, respectively. The results confirmed that the produced FeO-NPs were crystalline with a face-centered cubic structure based on the JCPDS No. 01-078- 6916(Fe_2O_3) and 01-071-6336 (Fe_3O_4). The detection of some peaks in the XRD chart indicates slight impurities associated with the scattering of plant-coated agents.

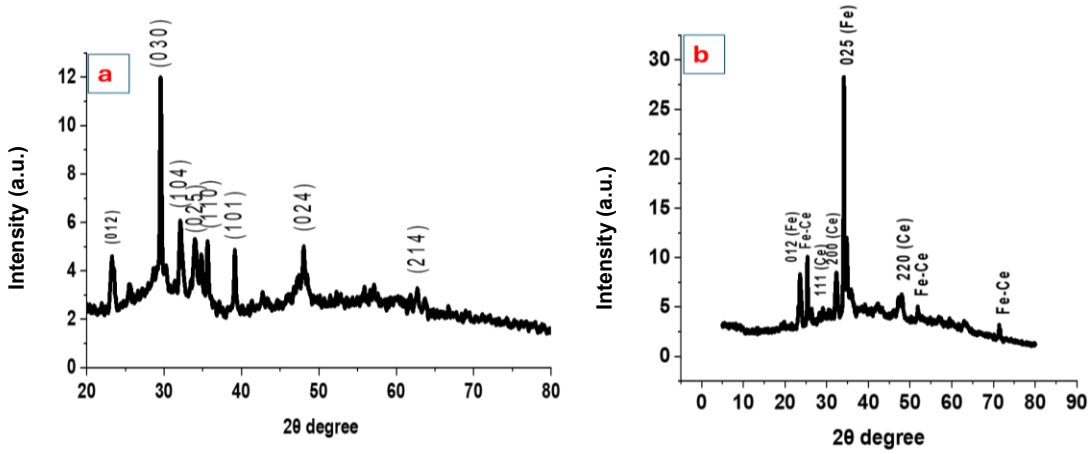

Fig. 3. XRD analysis of FeO NPs (a); and FeO/CeO NPs (b)

In Fig. 3b, new peaks related to CeO_2 NPs appeared at 2θ° values of 28.6° (111), 32.3° (200), 47.9° (220) (Balaji *et al*. 2020). Peaks also appeared at 2θ° values of 25.2°, 51.9°, and 71.5°, which may be related to bimetallic Fe/Ce NPs. The Debye‑Scherrer equation was utilized to determine the average crystallite size of nano-FeO based on XRD analysis. Analysis of the data revealed that the average crystallite size was 17.65 nm for iron oxide NPs (Fe_2O_{3+} Fe_3O_4) and 22.14 nm iron/cerium NPs (Fe_2O_{3+} Fe_3O_4/ CeO_2). In a similar study, the average nano-FeO crystallite size generated using *Egeria densa* extract ranged between 16.3 to 25.2 nm (Yekeen *et al*. 2025). A common cause of the discrepancy between XRD-derived crystallite sizes and TEM-observed particle sizes (tens of nm) is

that the particles are polycrystalline aggregates. A crystallite's size is measured by XRD, whereas the coherent scattering domain is measured by TEM. Aggregation, surface strain, polycrystalline structure, or amorphous layers are the causes of differences (Biehler and Abdel-Fattah (2025).

Antimicrobial Activity

The antibacterial activities of *Ficus nitida* extract, Fe-NPs, and Fe/Ce NPs were determined using the agar well diffusion method. Results are presented as mean inhibition zones (mm ± SE) in Table 1.

Table 1. Antimicrobial Activity of *Ficus nitida* Fruit Extract, Fe NPs, and Fe/Ce NPs

Microorganism	*Ficus nitida* Fruit Extract	Fe NPs	Fe/Ce NPs	Erythromycin	LSD (5%)
MRSA	12.5 ± 0.29c	18.5 ± 0.29b	21.0 ± 0.58a	0	2.32
B. cereus	11.0 ± 0.58c	15.5 ± 0.29a	16.0 ± 0.58a	13.8 ± 0.29b	1.65
S. aureus	12.8 ± 0.29b	12.7 ± 0.29b	15.8 ± 0.29a	13.0 ± 0.58b	2.15
K. pneumoniae	13.0 ± 0.58c	19.0 ± 0.58b	20.8 ± 0.44a	0	0.65
E. coli	0	19.8 ± 0.29b	22.2 ± 0.15a	0	1.19
A. baumannii	0	15.8 ± 0.29b	20.0 ± 0.58a	0	2.05

Significant differences are shown by different lowercase letters within a column that contain the same species (P≤0.05).

Both Gram-positive and Gram-negative bacterial strains, such as *Staphylococcus aureus*, *Bacillus cereus*, MRSA (Methicillin-resistant *Staphylococcus aureus*), *Escherichia coli, Klebsiella pneumoniae*, and *Acinetobacter baumannii*, were tested for the antibacterial activities of *Ficus nitida* fruit extract, Fe NPs, and bimetallic iron–cerium nanoparticles (Fe–Ce NPs). For statistical accuracy, Minitab software was used to compute the mean inhibition zones and standard errors (SE). The outcomes demonstrated distinct variations in sensitivity between the bacterial species studied.

The Fe–Ce NPs exhibited the highest antibacterial efficacy among all tested materials (Fig. 4), followed by Fe NPs and then *Ficus nitida* extract. The superior efficacy of Fe–Ce NPs likely results from synergistic Fe-Ce interactions that, as reported in recent literature, promote reactive oxygen species (ROS) generation and oxidative membrane damage (Radulescu *et al*. 2023; Manohar *et al*. 2024).

Among Gram-positive bacteria, MRSA and *Staphylococcus aureus* demonstrated strong sensitivity to Fe–Ce NPs, while *Bacillus cereus* showed comparatively lower inhibition zones. The significant inhibition observed against MRSA is particularly notable, as it indicates the potential of Fe–Ce NPs to combat multidrug-resistant pathogens that commonly evade conventional antibiotic treatment. The ROS produced by Fe–Ce NPs can bypass the classical β-lactam resistance mechanism by damaging the bacterial cell membrane directly and interfering with vital metabolic pathways. These findings highlight the capacity of Fe–Ce NPs to offer an alternative approach in managing resistant Gram-positive infections (Zhang and Miao 2024).

In the case of Gram-negative bacteria, *Acinetobacter baumannii* exhibited slightly lower inhibition zones than *Escherichia coli* and *Klebsiella pneumoniae*, consistent with its robust outer membrane and active efflux pump systems. However, the activity of Fe–Ce NPs against *Acinetobacter* remained significant, demonstrating their ability to generate oxidative stress, damage the bacterial envelope, and inhibit vital enzymatic functions. This suggests that Fe–Ce NPs can be effective even against difficult-to-treat nosocomial

pathogens such as *A. baumannii*, which pose major challenges in clinical environments (Kaushik *et al*. 2023; Al-Shimmary *et al*. 2025).

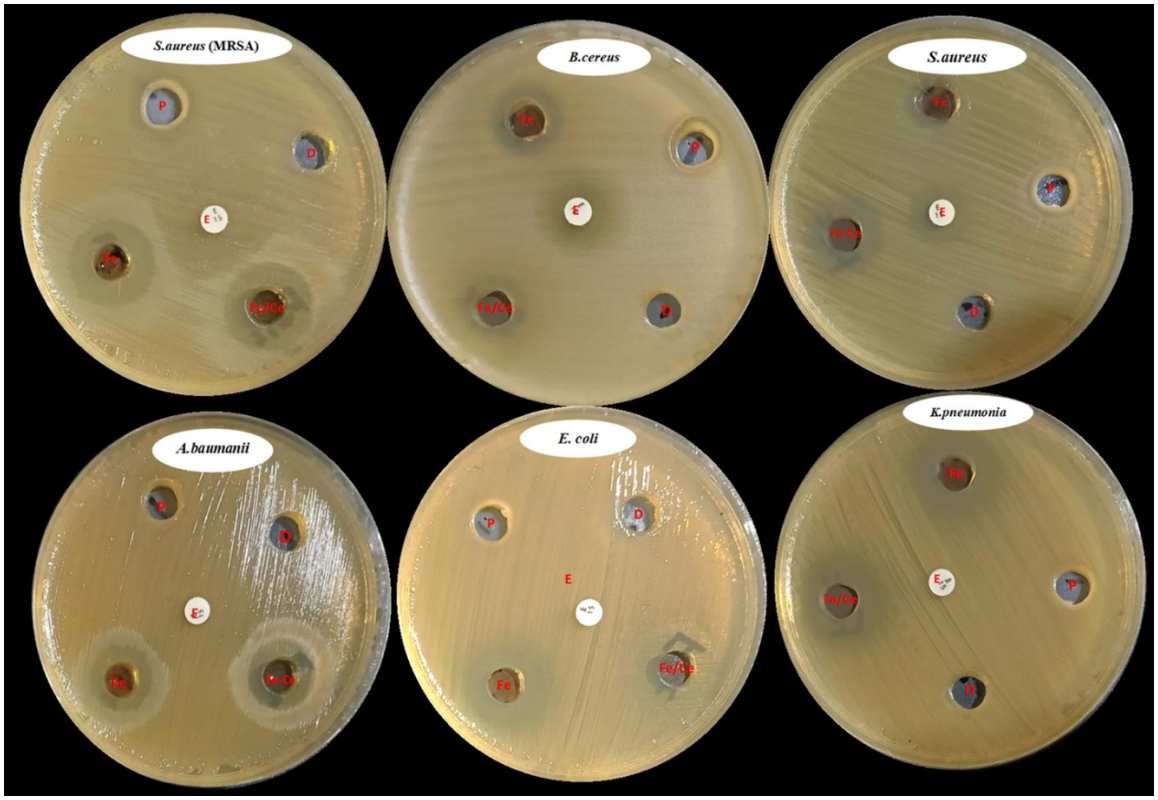

Fig. 4. Antimicrobial activity of (*Ficus nitida* fruit extract, Fe NPs, and Fe/Ce NPs) P = *Ficus nitida* fruit extract, Fe = FeNPs, Fe-Ce = Fe/Ce NPs, D = DMSO, E = Erythromycin 15 µg)

The comparison between Fe NPs and Fe–Ce NPs further demonstrates the importance of cerium addition. While Fe NPs alone exert antibacterial effects through Fenton-type reactions that produce hydroxyl radicals, the inclusion of Ce enhances the redox cycling capacity, prolonging ROS generation, and increasing stability. This combined mechanism explains the broader and more potent antibacterial activity observed for Fe–Ce NPs, particularly against MRSA and *A. baumannii*. The incorporation of Ce also reduces aggregation and enhances surface reactivity, further improving nanoparticle performance (Manohar *et al*. 2024).

The *Ficus nitida* fruit extract alone exhibited moderate antibacterial activity, attributed to the presence of phenolic compounds, flavonoids, and tannins capable of interacting with bacterial proteins and membranes. However, its role as a reducing and stabilizing agent in the green synthesis of NPs significantly enhanced antibacterial activity. The phytochemicals in the extract contribute to nanoparticle biofunctionalization, improving their stability, dispersity, and reactivity, thus increasing their effectiveness (El-Sayed *et al*. 2014; Rashed *et al*. 2018).

Overall, the findings confirm that green-synthesized Fe–Ce NPs using *Ficus nitida* extract are highly effective antibacterial agents against both Gram-positive and Gram-negative bacteria, including multidrug-resistant strains such as MRSA and *Acinetobacter baumannii*. Their strong antibacterial potential results from a combination of ROS generation, ion release, and bio functional surface interactions. Therefore, Fe–Ce NPs can

be proposed as promising candidates for future antimicrobial coatings, wound dressings, and pharmaceutical formulations designed to control resistant pathogens.

Determination of Minimum Inhibitory Concentration

Table 2 presenting the minimum inhibitory concentrations (MIC) of Fe NPs and Consortium (Fe/Ce NPs). Based on the provided data, the MIC values differ across bacterial strains (Fig. 5).

Table 2. Determination of MIC of Fe NPs, and Fe/Ce NPs against Multidrug Resistant Bacteria

Microorganism	Fe NPs	Fe/Ce NPs
MRSA	250 µg/mL	250 µg/mL
B. cereus	250 µg/mL	250 µg/mL
S. aureus	250 µg/mL	250 µg/mL
K. pneumoniae	250 µg/mL	125 µg/mL
E. coli	500 µg/mL	500 µg/mL
A. baumannii	250 µg/mL	250 µg/mL

Significant differences are shown by different lowercase letters within a column that contain the same species (P≤0.05).

In this experiment (Table 2, and Fig. 5), the MIC of Fe NPs and Fe/Ce NPs against multidrug-resistant bacteria was determined. As shown in the Table 2, the effect of both Fe-NPs and Fe/Ce NPs was tested against six different bacterial strains. The results indicate that Fe NPs and Fe/Ce NPs had similar effects against several bacterial strains, with MIC values of 250 µg/mL for MRSA, *B. cereus, S. aureus*, and *A. baumannii.* However, it was observed that Fe/Ce NPs had a stronger effect against *K. pneumoniae*, where the MIC value was lower at 125 µg/mL, compared to Fe-NPs, which showed a MIC value of 250 µg/mL. For *E. coli*, both Fe-NPs and Fe/Ce NPs showed higher MIC values of 500 µg/mL, indicating that this bacterium may be more resistant to these materials compared to the others in the study. These results suggest that the addition of Ce to Fe-NPs may improve their efficacy against certain bacterial strains, particularly *K. pneumoniae*, potentially due to the interaction between Fe and Ce that enhances antibacterial effects.

Antioxidant Activity of NPs

The DPPH assay demonstrated a clear concentration-dependent antioxidant activity for all tested samples, including Fe/Ce bimetallic NPs, Fe-NPs, and the reference antioxidant ascorbic acid (Fig. 6). As expected, ascorbic acid showed the highest scavenging activity across all concentrations, reaching 95.8% at 1000 µg/mL and maintaining strong activity even at the lowest concentration (49.6% at 7.81 µg/mL). Fe/Ce NPs showed moderate but significant activity, with maximum inhibition of 81.8% at 1000 µg/mL, gradually decreasing to 12.4% at the lowest concentration. The Fe NPs exhibited the lowest performance, starting at 79.2% inhibition at 1000 µg/mL and declining to 6.4% at 7.81 µg/mL.

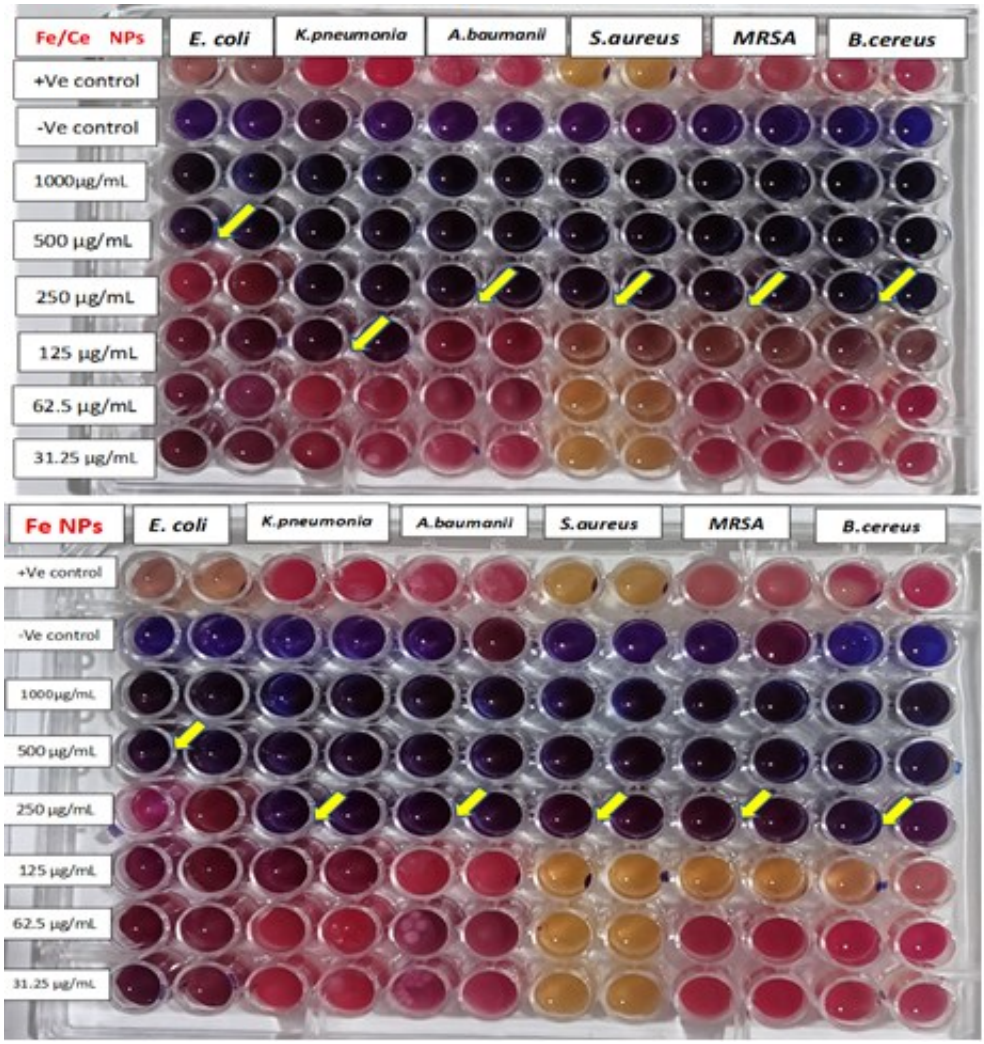

Fig. 5. MIC values of Fe-NPs, and Fe/Ce NPs on (*E. coli*, *K. pneumonia*, *S. aureus*, *B. cereus,* MRSA, and *A. baumannii*) plates after 24 h in Mueller Hinton (MH) broth resazurin assay [pink color indicates growth and blue means inhibition of growth, +Ve control (MH broth + bacterial suspension + indicator) without compounds; -Ve control = Sterility control (MH broth + sterile distilled water + indicator) without bacteria.

Overall, the order of antioxidant activity across all concentrations was: ascorbic acid > Fe/Ce NPs > Fe NPs. The superior antioxidant activity of ascorbic acid is consistent with its well-established role as a potent electron donor, rapidly quenching DPPH radicals through hydrogen-atom transfer mechanisms. In comparison, the enhanced performance of Fe/Ce NPs over Fe-NPs can be attributed to the synergistic redox properties of cerium, particularly the Ce^{3+}/Ce^{4+} redox pair known for its catalytic radical-scavenging capacity. This explains why Fe/Ce NPs maintained higher inhibition values than Fe-NPs at every concentration tested (Peera and Kim 2025). The Fe-NPs' reduced activity could be attributed to their lack of cerium-mediated regeneration cycles and more restricted surface reactivity. These results are in line with other studies that show enhanced antioxidant effectiveness in metal-oxide nanocomposites because of their larger surface area and capacity for multi-valence electron transfer. Therefore, adding Ce to Fe-NPs significantly increases their capacity to scavenge free radicals, yet neither formulation is as effective as ascorbic acid (Shah *et al*. 2017).

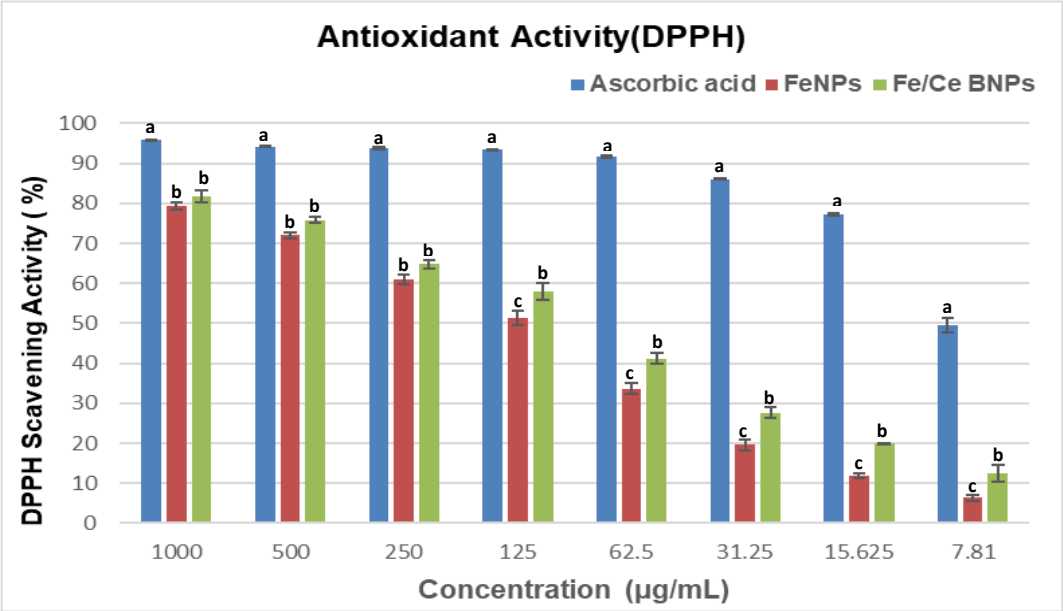

Fig. 6. Antioxidant activity of Fe NPs, and Fe/Ce NPs at different concentrations using DPPH method. Significant differences are shown by different lowercase letters within a column that contain the same species ($P \leq 0.05$).

CONCLUSIONS

1. *Ficus nitida* fruit aqueous extract successfully mediated green synthesis of FeO and FeO/CeO_2 nanoparticles (NPs) for the first time.
2. Synthesized NPs exhibited antibacterial activity against multi-drug resistant (MDR) clinical isolates and concentration-dependent antioxidant potential.
3. Transmission electron microscope (TEM) analysis confirmed irregular, spherical, and agglomerated morphologies for both FeO and FeO /CeO nanoparticle samples.
4. FeO/CeO_2 NPs demonstrated superior antibacterial efficacy (inhibition zones: 21.0 ± 0.58 mm *vs.* MRSA; 22.2 ± 0.15 mm vs *E. coli*) and DPPH scavenging 81.8% maximum at 1000 µg/mL and gradually decreasing to 12.4% at the lowest concentration.
5. The enhanced antibacterial performance of FeO/CeO_2 NPs suggests synergistic Fe-Ce interactions that may contribute to improved activity against certain MDR strains. Future studies should investigate Ce^{3+}/Ce^{4+} redox cycling mechanisms, mammalian cytotoxicity, and *in vivo* efficacy to validate biomedical potential.

ACKNOWLEDGMENTS

The authors extend their appreciation to the Princess Nourah bint Abdulrahman University Researchers Supporting Project number (PNURSP2026R891), Princess Nourah bint Abdulrahman University,Riyadh,Saudi Arabia. The authors extend their appreciation to the Deanship of Scientific Research at Northern Border University, Arar, KSA, for funding this research work through the project number "NBU-FFR-2026-337-01"

REFERENCES CITED

Abd-ElGawad, A. M., Amin, M. A., Ismail, M. A., Ismail, M. K., Radwan, A. A., Sarker, T. C., El-Naggar, M. A., and Abdelkareem, E. M. (2025). "Selenium/copper oxide nanoparticles prepared with *Urtica urens* extract: Their antimicrobial, antioxidant, antihemolytic, anticoagulant, and plant growth effects," *BioResources* 20(2), 2791-2810. https://doi.org/10.15376/biores.20.2.2791-2810

Abdelghany, T. M., Al-Rajhi, A. M. H., Yahya, R., Bakri, M. M., Al Abboud, M. A., Yahya, R., and Salem, S. S. (2023). "Phytofabrication of zinc oxide nanoparticles with advanced characterization and its antioxidant, anticancer, and antimicrobial activity against pathogenic microorganisms," *Biomass Conversion and Biorefinery* 13, 417-430. https://doi.org/10.1007/s13399-022-03412-1

Al-Shimmary, S. M., Shehab, Z. H., and Jassim, E. H. (2025). "Synthesis and characterization of cerium oxide-bacteriocin nanohybride with synergistic biological activities," *Egyptian Journal of Basic and Applied Sciences* 12(1), 1-16. https://doi.org/10.1080/2314808X.2024.2442250

Amin, M. A. A., Abu-Elsaoud, A. M., Nowwar, A. I., Abdelwahab, A. T., Awad, M. A., Hassan, S. E. D., and Elkelish, A. (2024). "Green synthesis of magnesium oxide nanoparticles using endophytic fungal strain to improve the growth, metabolic activities, yield traits, and phenolic compounds content of *Nigella sativa* L," *Green Processing and Synthesis* 13(1), article 20230215. https://doi.org/10.1515/gps-2023-0215

Amin, M. A., Algamdi, N. A., Waznah, M. S., Bukhari, D. A., Alsharif, S. M., Alkhayri, F., Abdel-Nasser, M. and Fouda, A. (2025). "An insight into antimicrobial, antioxidant, anticancer, and antidiabetic activities of trimetallic Se/ZnO/CuO nanoalloys fabricated by aqueous extract of *Nitraria retusa*," *Journal of Cluster Science* 36(1), 1-15. https://doi.org/10.1007/s10876-024-02742-6

Balaji, S., Mandal, B. K., Vinod Kumar Reddy, L., and Sen, D. (2020). "Biogenic ceria nanoparticles (CeO_2 NPs) for effective photocatalytic and cytotoxic activity," *Bioengineering* 7(1), article 26. https://doi.org/10.3390/bioengineering7010026

Basu, T., Nandi, D., Sen, P., and Ghosh, U. C., (2013). "Equilibrium modeling of As (III, V) sorption in the absence/presence of some groundwater occurring ions by iron (III)-cerium (IV) oxide nanoparticle agglomerates: a mechanistic approach of surface interaction," *Chem. Eng. J.* 228, 665-678. https://doi.org/10.1016/j. cej.2013.05.037

Biehler, E., and Abdel-Fattah, T. M. (2025). "Glucose-mediated synthesis of spherical carbon decorated with gold nanoparticles as catalyst in a hydrogen generation reaction," *Catalysts* 15(12), article 1141. https://doi.org/10.3390/catal15121141

Chen, Z., Yu, G., and Wang, Q. (2020). "Effects of climate and forest age on the ecosystem carbon exchange of afforestation," *Journal of Forestry Research* 31(2), 365-374. https://doi.org/10.1007/s11676-019-00946-5

Demirezen, D. A., Yıldız, Y. Ş., Yılmaz, Ş., and Yılmaz, D. D. (2019). "Green synthesis and characterization of iron oxide nanoparticles using *Ficus carica* (common fig) dried fruit extract," *Journal of Bioscience and Bioengineering* 127(2), 241-245. https://doi.org/10.1016/j.jbiosc.2018.07.024

Dikshit, P. K., Kumar, J., Das, A. K., Sadhu, S., Sharma, S., Singh, S., Gupta, P. K., and Kim, B. S. (2021). "Green synthesis of metallic nanoparticles: Applications and limitations," *Catalysts* 11(8), article 902. https://doi.org/10.3390/catal11080902

El-Batal, A. I., Ismail, M. A., Amin, M. A., El-Sayyad, G. S., and Osman, M. S. (2023). "Selenium nanoparticles induce growth and physiological tolerance of wastewater-stressed carrot plants," *Biologia* 78(9), 2339-2355. https://doi.org/10.1007/s11756-023-01401-x

El-Didamony, S. E., Kalaba, M. H., Sharaf, M. H., El-Fakharany, E. M., Osman, A., Sitohy, M., and Sitohy, B. (2024). "Melittin alcalase-hydrolysate: A novel chemically characterized multifunctional bioagent; antibacterial, anti-biofilm and anticancer," *Frontiers in Microbiology* 15, article 1419917. https://doi.org/10.3389/fmicb.2024.1419917

El-Sayed, M. H., Refaat, B. M., and Sharaf, M. H. (2014). "Microbiological evaluation of antibacterial potentiality of some edible plant extracts against multidrug resistant (MDR) human pathogens," *International Current Pharmaceutical Journal* 4(1), 336-339. https://doi.org/10.3329/icpj.v4i1.21162

El-Sayed, M. H., Alshammari, F. A., and Sharaf, M. H. (2023). "Antagonistic potentiality of actinomycete-derived extract with anti-biofilm, antioxidant, and cytotoxic capabilities as a natural combating strategy for multidrug-resistant ESKAPE pathogens," *Journal of Microbiology and Biotechnology* 33(1), article 61. https://doi.org/10.4014/jmb.2211.11026

Kaushik, A., Singh, R. K., and Tyagi, P. K. (2023). "Green synthesized nanoparticle based drug delivery: Recent trends and future prospects," *Precision Nanomedicine* 6(4), 1109-1131. https://doi.org/10.33218/001c.89165

Manohar, A., Suvarna, T., Vattikuti, S. P., Sudhani, H. P., Manivasagan, P., Jang, E. S., Al-Asbahi, B. A., Mameda, N., and Kim, K. H. (2024). "Ternary nanocomposites of $ZnFe_2O_4$/$NiFe_2O_4$/CeO_2: investigating electrochemical energy storage and biocompatible properties," *Journal of Environmental Chemical Engineering* 12(5), article 113337. https://doi.org/10.1016/j.jece.2024.113337

Mohamed, A. E., Elgammal, W. E., Eid, A. M., Dawaba, A. M., Ibrahim, A. G., Fouda, A., and Hassan, S. M. (2022). "Synthesis and characterization of new functionalized chitosan and its antimicrobial and *in-vitro* release behavior from topical gel," *International Journal of Biological Macromolecules* 207, 242-253. https://doi.org/10.1016/j.ijbiomac.2022.02.173

Nadeem, M., Khan, R., Shah, N., Bangash, I. R., Abbasi, B. H., Hano, C., Liu, C., Ullah, S., Hashmi, S.S., Nadhman, A., and Celli, J. (2021). "A review of microbial mediated iron nanoparticles (IONPs) and its biomedical applications," *Nanomaterials* 12(1), article 130. https://doi.org/10.3390/nano12010130

Pedroso-Santana, S., and Fleitas-Salazar, N. (2023). "The use of capping agents in the stabilization and functionalization of metallic nanoparticles for biomedical applications," *Particle & Particle Systems Characterization* 40(2), article 2200146.

Peera, S. G., and Kim, S. W. (2025). "Rare earth Ce/CeO_2 electrocatalysts: Role of high electronic spin state of Ce and Ce^{3+}/Ce^{4+} redox couple on oxygen reduction reaction," *Nanomaterials* 15(8), article 600. https://doi.org/10.3390/nano15080600

Qi, M., Li, W., Zheng, X., Li, X., Sun, Y., Wang, Y., Li, C., and Wang, L. (2020). "Cerium and its oxidant-based nanomaterials for antibacterial applications: A state-of-the-art review," *Frontiers in Materials* 7, article 213.

Salih, K. A., Zhou, K., Hamza, M. F., Mira, H., Wei, Y., Ning, S., Guibal, E., and Salem, W. M. (2023). "Phosphonation of alginate–polyethyleneimine beads for the enhanced removal of cs (I) and Sr (II) from aqueous solutions," *Gels* 9(2), article 152.

Selim, S., Almuhayawi, M. S., Alruhaili, M. H., Tarabulsi, M. K., Saddiq, A. A., Elamir, M. Y. M., Amin, M. A., and Al Jaouni, S. K. (2025a). "Pharmacological applications and plant stimulation under sea water stress of biosynthesis bimetallic ZnO/MgO NPs," *Scientific Reports* 15(1), article 5263. https://doi.org/10.1038/s41598-025-87881-0

Selim, S., Saddiq, A. A., Ashy, R. A., Baghdadi, A. M., Alzahrani, A. J., Mostafa, E. M., Al Jaouni, S. K., Elamir, M. Y. M., Amin, M. A., Salah, A. M., *et al.* (2025b). "Bimetallic selenium/zinc oxide nanoparticles: Biological activity and plant biostimulant properties," *AMB Express* 15(1), 1-11. https://doi.org/10.1186/s13568-024-01808-y

Shah, S. T., Yehye, W. A., Saad, O., Simarani, K., Chowdhury, Z. Z., Alhadi, A. A., and Al-Ani, L. A. (2017). "Surface functionalization of iron oxide nanoparticles with gallic acid as potential antioxidant and antimicrobial agents," *Nanomaterials* 7(10), article 306. https://doi.org/10.3390/nano7100306

Radulescu, D. M., Surdu, V. A., Ficai, A., Ficai, D., Grumezescu, A. M., and Andronescu, E. (2023). "Green synthesis of metal and metal oxide nanoparticles: A review of the principles and biomedical applications," *International Journal of Molecular Sciences* 24 (20), article 15397. https://doi.org/10.3390/ijms242015397

Rashed, K., Lai, C. S., Pan, M. H., and Feitosa, C. (2018). "Study of the antioxidant and anti-inflammatory potential of the aerial parts of *Ficus nitida* L.(Moraceae) and its phytochemical composition," *Jordan Journal of Pharmaceutical Sciences* 11(2).

Rego, R. M., Sriram, G., Ajeya, K. V., Jung, H. Y., Kurkuri, M. D., and Kigga, M. (2021). "Cerium based UiO-66 MOF as a multipollutant adsorbent for universal water purification," *Journal of Hazardous Materials* 416, article 125941. https://doi.org/10.1016/j.jhazmat.2021.125941

Sharaf, M. H., El-Sherbiny, G. M., Moghannem, S. A., Abdelmonem, M., Elsehemy, I. A., Metwaly, A. M., and Kalaba, M. H. (2021). "New combination approaches to combat methicillin-resistant *Staphylococcus aureus* (MRSA)," *Scientific Reports* 11(1), 1-16. https://doi.org/10.1038/s41598-021-82550-4

Shreyash, N., Bajpai, S., Khan, M. A., Vijay, Y., Tiwary, S. K., and Sonker, M. (2021). "Green synthesis of nanoparticles and their biomedical applications: A review," *ACS Applied Nano Materials* 4(11), 11428-11457. https://doi.org/10.1021/acsanm.1c02946

Singh, H., Desimone, M. F., Pandya, S., Jasani, S., George, N., Adnan, M., Abdu Aldarhami , Bazaid, A. s., and Alderhami, S. A. (2023). "Revisiting the green synthesis of nanoparticles: uncovering influences of plant extracts as reducing agents for enhanced synthesis efficiency and its biomedical applications," *International Journal of Nanomedicine* 4727-4750. https://doi.org/10.2147/IJN.S419369

Sriram, G., Bendre, A., Altalhi, T., Jung, H. Y., Hegde, G., and Kurkuri, M. (2022).

"Surface engineering of silica based materials with Ni–Fe layered double hydroxide for the efficient removal of methyl orange: Isotherms, kinetics, mechanism and high selectivity studies," *Chemosphere* 287, article 131976. https://doi.org/10.1016/j.chemosphere.2021.131976

Vijayaram, S., Razafindralambo, H., Sun, Y. Z., Vasantharaj, S., Ghafarifarsani, H., Hoseinifar, S. H., and Raeeszadeh, M. (2024). "Applications of green synthesized metal nanoparticles—A review," *Biological Trace Element Research* 202(1), 360-386. https://doi.org/10.1007/s12011-023-03645-9

Yekeen, M. O., Ibrahim, M., Wachira, J., and Pramanik, S. (2025). "Green synthesis and characterization of iron oxide nanoparticles using *Egeria densa* plant extract," *Applied Biosciences* 4(2), article 27. https://doi.org/10.3390/applbiosci4020027

Zhang, T. G., and Miao, C. Y. (2024). "Iron oxide nanoparticles as promising antibacterial agents of new generation," *Nanomaterials* 14(15), article 1311. https://doi.org/10.3390/nano14151311

Zamani, K., Allah-Bakhshi, N., Akhavan, F., Yousefi, M., Golmoradi, R., Ramezani, M., Bach, H., Razavi, S., Irajian, G., Gerami, M., Pakdin-Parizi, A., Tafrihi, M., and Ramezani, F. (2021). "Antibacterial effect of cerium oxide nanoparticle against *Pseudomonas aeruginosa*," *BMC Biotechnology* 21(1), article 68. https://doi.org/10.1186/s12896-021-00727-1

Article submitted: November 22, 2025; Peer review completed: January 30, 2026; Revised version received and accepted: February 18, 2026; Published: March 2, 2026.
DOI: 10.15376/biores.21.2.3673-3687